Conclusions. 1. In superrapid hardening in the layer remelted in laser irradiation of originally nonhomogeneous $Fe_{83}B_{17}$ alloy three areas are formed, inclusions of α-iron crystals, an amorphous zone, and an intermediate boron-enriched layer.

2. Crystallization of the amorphous areas obtained in laser treatment occurs in more than one stage in a broad temperature range. With an increase in the number of laser irradiations the thermal stability of the amorphous areas decreases.

LITERATURE CITED

1. P. L. Gruzin, A. A. Kasimovskii, E. E. Goncharov, et al., "The physical processes in laser amorphization of Fe—B and Fe—Si—B alloys," in: Amorphous Metallic Materials [in Russian], Nauka, Moscow (1984), pp. 135-139.
2. A. A. Kasimovskii, "The structure of the surface layer of iron and silicon-base alloys after ion and laser treatment investigated by the nuclear gamma resonance method," Candidate's Thesis, Physicomathematical Sciences, Moscow (1985).
3. Yu. V. Petrikin, V. A. Bychkov, A. A. Kasimovskii, et al., "A gas-discharge detector for electron nuclear gamma resonance spectroscopy," Zavod. Lab., 49, No. 11, 46-48 (1983).
4. Yu. A. Skakov and V. S. Kraposhin, "Solidification under conditions of superrapid cooling," in: The Results of Science and Technology. Metal Science and Heat Treatment [in Russian], Vol. 13, Vsesoyuz. Inst. Nauch. i Tekh. Inf., Moscow (1980), pp. 3-78.
5. T. Kemeny, I. Vincze, B. Fogarassy, et al., "Structure and crystallization of Fe—B metallic glasses," Phys. Rev., 20, No. 2, 476-488 (1979).
6. D. E. G. Williams, D. E. Sykes, and H. Fujimori, "Auger studies of $Fe_{4.7}Co_{70.3}Si_{15}B_{10}$," in: Proceedings of the Fourth International Conference on Rapidly Quenched Metals, August 24-28, 1981, Sendai, Japan, Vol. 2 (1982), pp. 1483-1484.
7. T. I. Bratus', M. A. Vasil'ev, and V. T. Cherepin, "An investigation of the surface of $Fe_{80}B_{20}$ and $Fe_{40}Ni_{40}P_{16}B_4$ amorphous alloys by the method of electron Auger spectroscopy," Metallofizika, 5, No. 1, 71-75 (1983).

PROPERTIES OF ALLOY MA21 AFTER LASER TREATMENT

R. Kh. Kalimullin, V. B. Spiridonov, A. T. Berdnikov, A. A. Romanov, and G. N. Pautkina

UDC 621.9.048.7:669.721.5'884

The authors of [1-5] presented experimental data on the improvement of the anticorrosive and mechanical properties of the alloy MA21 of the system Mg—Li attained by laser treatment. However, these publications do not contain reports on detailed investigations of the regimes of laser heat treatment (LHT) that would make it possible to establish a correlation between the parameters of the treatment, the structure and properties of the material, which would be important to industry.

Moreover, there is no metal science analysis of the different structural states obtained in continuous (CLHT) and pulsed (PLHT) laser heat treatment.

On the basis of an analysis of the diffusion processes occurring during crystallization, the conclusion was reached that pure metal and alloys of eutectic type are most sensitive to the cooling rate [6].

In superrapid quenching by the method of pouring molten copper alloys of eutectic composition on a drum, the authors of [7] found five types of microstructures: from coarsely lamellar eutectic to single-phase metastable solid solution, and in the extreme case with a cooling rate of approximately 10^7 °K/sec, to a radiographically amorphous structure of solid solution.

Production Association "UralAZ."

Translated from Metallovedenie i Termicheskaya Obrabotka Metallov, No. 5, pp. 18-24, May, 1988.

0026-0673/88/0506-0000$12.50

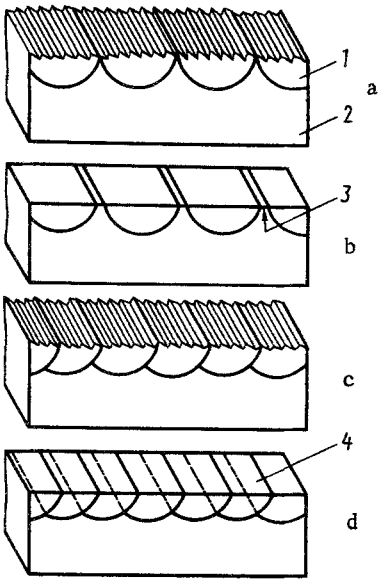

Fig. 1

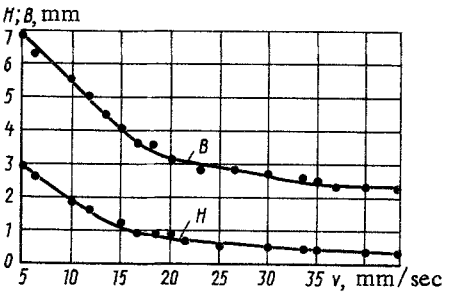

Fig. 2

Fig. 1. Diagram of the zones treated by continuous laser: a, b) without overlapping of the laser tracks; c, d) with overlapping of the laser tracks; 1) fused zone; 2) initial metal; 3) sections of initial structure after machining of the surface; 4) zone of overlapping laser tracks.

Fig. 2. Dependence of depth H and width B of the laser track on the speed with which the continuous beam is shifted, with $q = 0.4 \cdot 10^8$ W/m^2.

We therefore attempt in the present work to shed light on the regularities of the formation of some type of microstructure in the alloy MA21 under conditions of cooling after LHT; to reveal the effect of the principal parameters of irradiation on its properties, and to examine problems of optimization of the technological process of CLHT.

The investigations were carried out with rectangular specimens, 10 × 10 × 10, 20 × 20 × 30, 30 × 20 × 30, and 10 × 30 × 100 mm in size, of alloy MA21 in the hot-pressed state, obtained under industrial conditions in the form of formed semiproducts. Before the specimens were irradiated, their surface was provided with a light-absorbing coating in the form of an oxide film; this was done by a chemical method (in a solution consisting of 70 g/liter potassium chromate, 40 g/liter magnesium sulfate, and 50 g/liter ammonium sulfate).

The CLHT was carried out with the aid of a gas CO_2 laser with a power of up to 1 kW with wavelength of the radiation 10.6 μm. The diameter of the focused beam was measured on specimens of alloy MA21 coated with lubricant MTsS-10, with the radiation acting for 1 to 5 sec. The principal controlled parameters were the power density of the radiation (q) and the speed with which the surface of the alloy moved under the beam (v). The power density was changed within the limits $1.2 \cdot 10^7 \leqslant q \leqslant 1.6 \cdot 10^8$ W/m^2, the speed of the shifting $5 \cdot 10^{-3} \leqslant v \leqslant 4.3 \times 10^{-2}$ m/sec.

As a result we obtained a molten layer with different geometry, i.e., a laser "track" with a certain width B and depth H, ensuring different cooling rates of the melt.

To obtain a fused layer on the surface of the specimen that was uniform across its thickness, we carried out the treatment with overlapping of the laser tracks as shown in Fig. 1.

To optimize the parameters of CLHT it is necessary to determine the permissible temperature ΔT_p to which the alloy may be heated (the difference between the temperature of the heating and the normal one) at which light absorption of the surface increases and the stability of the technological process of irradiation is impaired. With the object of determining ΔT_p, we simulated the heating entailed in CLHT by preliminarily heating the specimens in a crucible. The temperature was continuously checked with the aid of a thermocouple and a portable potentiometer PP-63. The final temperature was changed between 25 and 320°C in

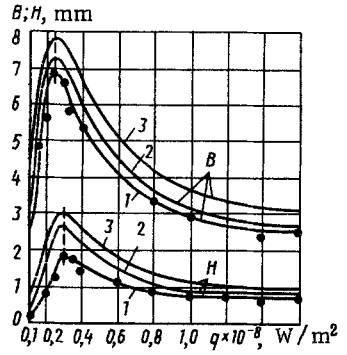

Fig. 3

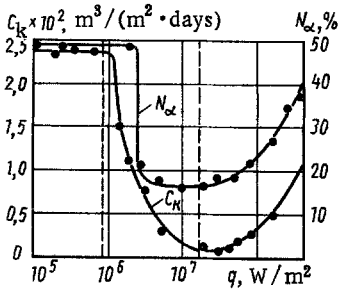

Fig. 4

Fig. 3. Dependence of depth H and width B of the laser track on the power density of the radiation with different speeds of shifting: 1) $v = 5 \cdot 10^{-3}$ m/sec; 2) $v = 6.6 \cdot 10^{-3}$ m/sec; 3) $v = 1.2 \cdot 10^{-2}$ m/sec.

Fig. 4. Effect of the power density of the radiation q on the corrosion rate C_k and the volume fraction of the α-phase N_α of the alloy MA21 ($v = 1.2 \cdot 10^{-2}$ m/sec).

steps of 5-10°C. After the specified temperature had been reached, the specimens were irradiated in the same optimal regime. Then we made metallographic sections and measured the width B and the depth H of the laser track, investigated the microstructure, and determined the corrosion rate for each temperature. From the jumplike change of the above-mentioned parameters we determined ΔT_p.

The energy parameters of CLHT do not suffice for obtaining an amorphous structure in the alloy MA21, we therefore used a solid-state pulsed glass laser with neodymium "Kvant-16." The generator operates in multimode regime: pulse energy up to 30 J, pulse width 3-6 msec, wavelength of the radiation 1.06 μm, beam diameter 2 mm. The pulse energy was changed within the limits $2.3 \leqslant E \leqslant 15$ J. The power density was varied within the limits $2.3 \cdot 10^9 \leqslant q \leqslant 1.5 \times 10^{10}$ W/m². Moreover, to increase the temperature gradient, we applied PLHT of the alloy MA21 in a medium of liquid nitrogen. Irradiation was carried out in a special device designed to prevent nitrogen vapors from reaching the irradiated surface.

After CLHT and PLHT the specimens were heated to 90°C with holding for 12 h, to 160°C with holding for 16 h, and to 100°C with holding for 100 h.

The methods of corrosion and microstructural investigations are described in [1-5]. However, it should be noted that in quantitative analysis of the microstructure on an analyzer Quantimet-720 we determined the mean volume fraction of the α-phase (%), viz. N_α. The microstructure and properties of the alloy were investigated in a separate spot or laser track as well as in a section irradiated with overlapping of the spots and tracks.

In dependence on the treatment regimes, CLHT of the surface of specimens of alloy MA21 leads to different results.

When the beam is shifted with increased speed, with q = const, H and B of the laser track decrease proportionately (Fig. 2). A similar dependence was obtained by many authors, e.g., [8]. Of greatest interest were the dependences H = f(q) and B = f(q) (Fig. 3). With

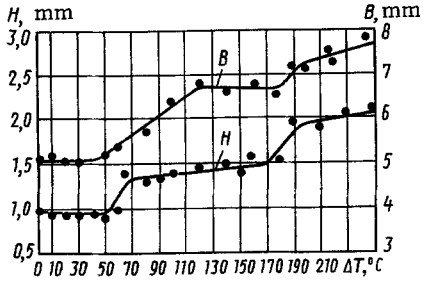

Fig. 5. Effect of the temperature ΔT to which the alloy MA21 is preliminarily heated in continuous laser treatment on the depth H and the width B of the laser track.

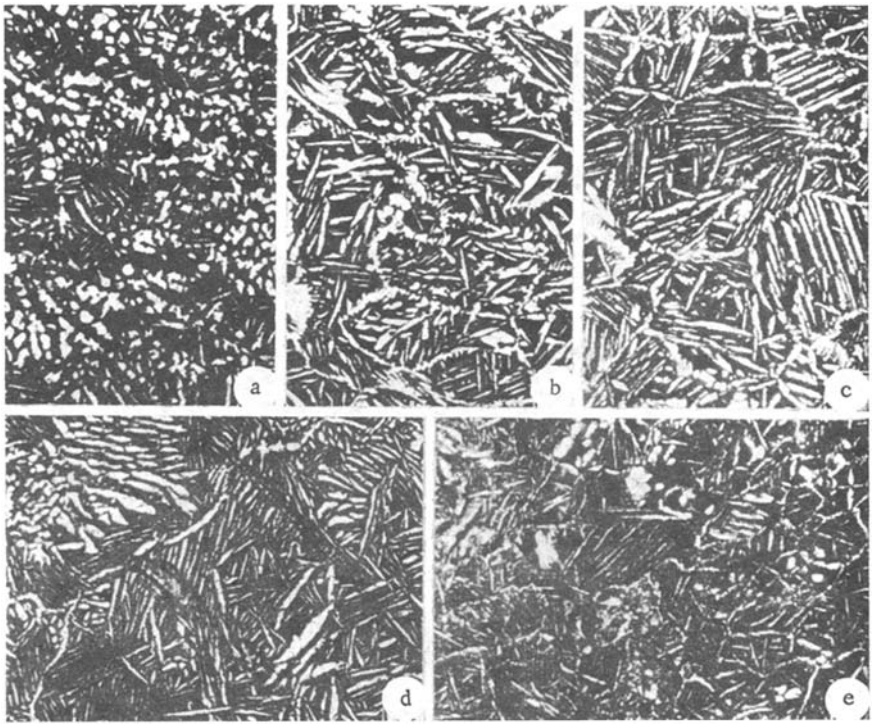

Fig. 6. Microstructure of alloy MA21 after continuous laser irradiation with speed of shifting $v = 10^{-2}$ m/sec and different power density of the radiation (×300): a) $q = 0.2 \cdot 10^8$ W/m^2; b) $0.4 \cdot 10^8$ W/m^2; c) $0.6 \cdot 10^8$ W/m^2; d) $0.8 \cdot 10^8$ W/m^2; e) $1.6 \cdot 10^8$ W/m^2.

$q \simeq 0.3 \cdot 10^8$ W/m^2 the curves have a maximum. This is obviously connected with various mechanisms of interaction of the continuous beam with the surface.

The values of q up to $0.3 \cdot 10^8$ W/m^2 lie below the threshold of developed evaporation and the threshold of plasma formation, part of the radiation is therefore expended on heating and melting the material, and part is reflected by the surface. With $q > 0.3 \cdot 10^8$ W/m^2 there is developed evaporation, and the energy contribution apparently suffices for the formation of a plasma flare. In our case the products of evaporation and the plasma defocus the radiation substantially. It is obvious that an increase of q entails an increased degree of defocusing, and this also causes a decrease of H.

In the investigation of the effect of the regimes of CLHT on the corrosion resistance it was established that it depends to a considerable extent on the specific energy contribution (Fig. 4). The lowest corrosion rate was found with $10^7 < q < 10^8$ W/m^2.

Preliminary heating of the alloy in CLHT causes a change of the structure and properties of the fused layer. The results of the investigation showed that in the investigated temperature range of preliminary heating there is a jumplike increase of H and B (Fig. 5).

The dependences $H = f(\Delta T)$ and $B = f(\Delta T)$ are well correlated with the results of [9] where it was shown that the absorption coefficient increases periodically jumplike when the copper target in continuous irradiation is heated to higher temperatures. It is obvious that the pulsations of light absorption are due primarily to the jumplike growth of the oxide film on the surface of the alloy [10].

To describe the structural changes occurring in the alloy MA21 in CLHT in different regimes, we used A. A. Bochvar's classification of eutectic structures which was presented sufficiently completely in [11].

The general nature of the microstructures revealed by the methods of optical metallography corresponds fully to those observed by the authors of [7]. In the initial state the alloy has a conglomerate structure consisting of α-phase and β-phase [1-5].

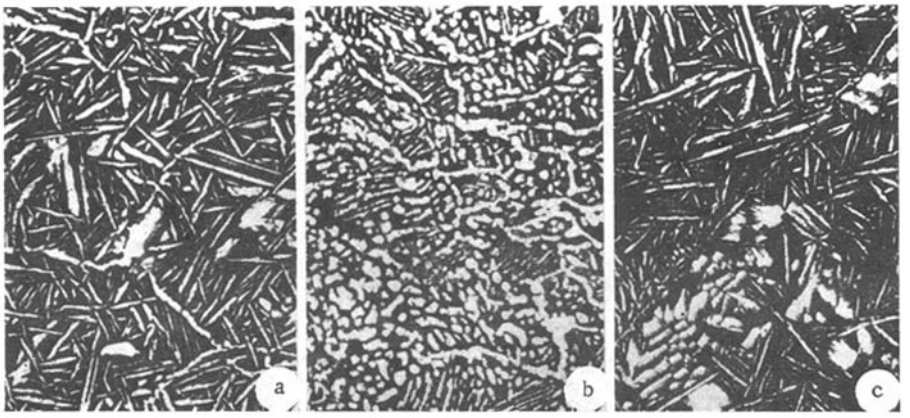

Fig. 7. Modifications of the quasieutectic structure after continuous laser irradiation of rectangular platelets (10 × 20 × 30 mm, 10 × 20 × 100 mm) of alloy MA21 (×300): a) acicular; b) acicular—globular; c) acicular structure + primary crystals.

The microstructure obtained in different regimes of CLHT is fine-grained quasieutectic with different micromorphology, i.e., phase composition in the form of needles, lamellas, globules (Fig. 6). The phase composition of the alloy remains practically unchanged. However, x-ray diffraction analysis showed that the ratio of the lattice parameters of the irradiated alloy is larger ($c/a \cong 1.8317$), than of the initial one ($c/a \cong 1.5535$). The micromorphology of the alloy in the zone affected by the continuous laser beam depends to a considerable extent on the energy contribution. Thus, a quantitative analysis showed that with different q in the zone of crystallization of the melt there occurs a regular change of the ratio of volume fractions of the α- and β-phases (see Fig. 4). The nature of the change of the volume fraction of α-phase is analogous to the change of C_k in dependence on q. The authors of [11] ascribed the change of the quantitative ratio of α- and β-phases in the process of crystallization to uncompensated opposed diffusion flows as a result of which one of the phases suffers constantly from lack of building material, and the surface of its crystallization front decreases. If we bear in mind that the diffusion coefficient of lithium in the melt is larger than the diffusion coefficient of magnesium and other elements, it is obvious that ahead of the β-front there is oversaturation with lithium atoms which causes an increase of the volume fraction of the β-phase.

In metallographic investigations it was established that the formation of some quasieutectic structure in the zone of irradiation is affected by the geometric shape of the specimen. Thus, in the zone of irradiation of the end face of the specimen 30 × 30 × 40 mm in size, with $H = 5 \cdot 10^{-4}$ m, the microstructure of the fused layer is globular quasieutectic only. With $H > 5 \cdot 10^{-4}$ m the fused layer consists of two or three zones with different micromorphology, as was shown in [4]. With $H > 1.5 \cdot 10^{-3}$ m the microstructure of the layer across the section consists of acicular quasieutectic.

The results of irradiation of platelets 10 × 20 × 30 mm and 10 × 20 × 100 mm showed that there is no regularity governing the formation of the microstructure of some micromorphology. In the fused layer we found different sections with acicular or globular, often with mixed globular and acicular structure (Fig. 7). In addition to that, in some cases we also found segregation of primary crystals. It is probable that the formation of such different structures in the zone of fusion is connected with the nonsteady distribution of heat fluxes. In

TABLE 1

H, μm	c/a	
	α′-Mg	α-Mg
0	1,6045	1,6083
50	1,6072	1,6093
110	1,6061	1,6048
160	1,6110	1,6059
400	—	1,6051

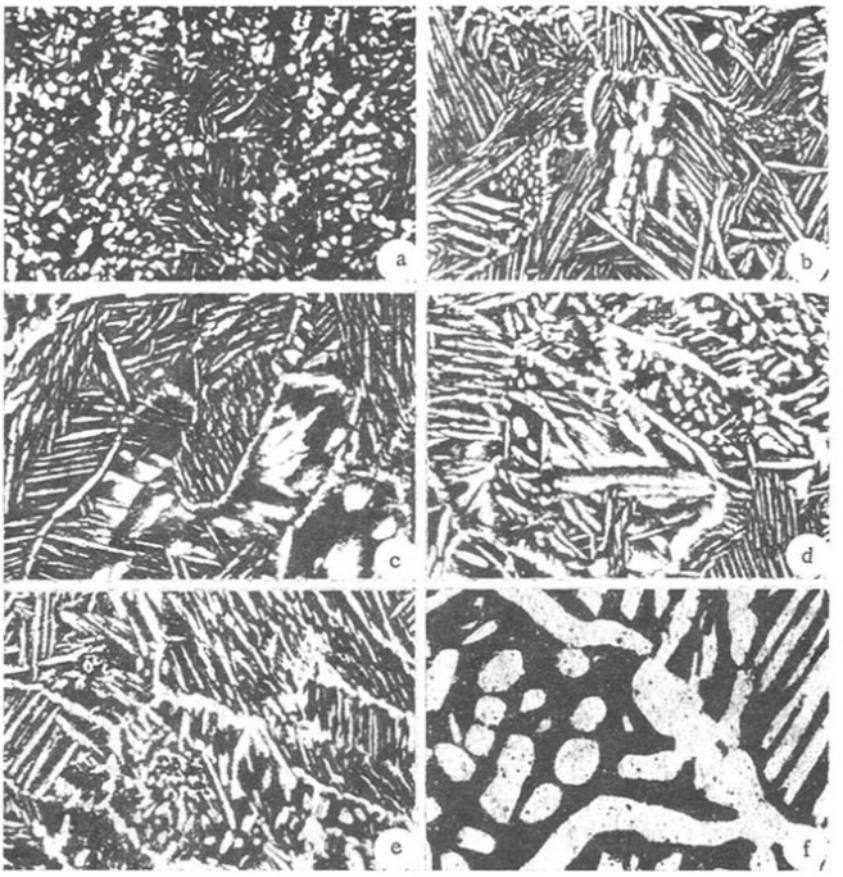

Fig. 8. Microstructure of alloy MA21 after preliminary heating to different temperatures under continuous irradiation (×300): a) ΔT = 5°C; b) 35°C; c) 65°C; d) 95°C; e) 200°C; f) 250°C.

irradiation the secondary heat fluxes, being reflected by different sides of the specimen, determine the process of formation of quasieutectic. However, when specimens 30 mm thick or thicker are irradiated, the heat fluxes apparently do not have sufficient time to affect the process of eutectic crystallization, and the structure in the fused zone is therefore stable.

Of interest are the phase transformations occurring in the structure of the fused layer at different temperatures to which the material is preliminarily heated. With rising temperature we find a noticeable increase of the dimensions of the phase components. At ΔT_p = 60-70°C primary α-crystals segregated; their dimensions were considerably larger than those of particles of α- and β-phases. This indicates that when the cooling rate is reduced, preliminary heating of the alloy entails its hypoeutectic crystallization in the zone of fusion (Fig. 8).

A quantitative analysis of the structure with different ΔT showed that when the material is heated to higher temperatures, the volume fraction of α-phase increases and is maximal (N_α = 36.8%) with ΔT = 200°C. It can be seen from Fig. 9 that N_α increases when $\Delta T \geqslant 60$ °C. On the whole, the nature of the dependence $N_\alpha = f(\Delta T)$ is analogous to $C_k = f(\Delta T)$.

The results of a quantitative analysis make it possible to explain the change of corrosion resistance of the alloy with different q and ΔT. The sections of α-phase in the alloy MA21 are cathodic in relation to β-phase. In consequence and in accordance with the laws of electrochemical kinetics, an increase of their amount causes an increase of the rate of anodic dissolution of β-phase, and conversely, a decrease of α-phase slows down the anodic process.

Processing of the experimental results, which was done on a computer, consisted in the numerical determination of the functions $H = f(v, q)$, $B = f(v, q)$, $C_k = f(q)$, $N_\alpha = f(q)$ for correlation with the experimental data. In the analysis of the obtained results we

TABLE 2

Treatment	Regime of subsequent heating	$C_k \cdot 10^3$, $m^3/(m^2 \cdot days)$
Initial state	Without heating 100 °C 100 h 160 °C 16 h	2,4 . 3,0
CLHT ($q = 0.4 \cdot 10^8$ W/m^2, $v = 10^{-2}$ m/sec)	Without heating 100 °C 100h 160 °C 16 h	0,65 . 0,85/0,35...0,45 0,7 ..0,95/0,4...0,5 0,8...1,0/0,4. 0,5
PLHT (E = 15 J, d = 3 mm)	Without heating 100 °C 100 h 160 °C 16 h	1,5. 1,8/0,12...0,16 6,0.. 7,5/0,18...0,23 5,8...7,2/—

Note. The numerator gives the corrosion rate after irradiation with overlapping, the denominator without overlapping.

approximated the descending branch of the curve in Fig. 3 and the ascending one in Fig. 4. As a result we obtained dependences of logarithmic type, i.e., the system of equations:

$$H_v = 4.109 - 2.932 \lg v;$$
$$H_q = 0.839 - 1,618 \lg q;$$
$$B_v = 9.351 - 5.366 \lg v;$$
$$B_q = 3.371 - 4,568 \lg q;$$
$$C_k = 0.431 + 0.779 \lg q;$$
$$N_\alpha = 12,891 + 12,230 \lg q$$

In the zone affected by the pulsed laser the phase structure was not revealed by etching. We found the microstructure of solid solution with the characteristic network of grain boundaries. The grain size was 1-15 μm (Fig. 10). The coarsest grains were situated at the center of the spot, toward the periphery the grain became smaller. In the zone of pulsed irradiation microhardness was H 820-850* compared with H 300-350 in the initial state and H 720-740 after CLHT. When we investigated the transverse layer, we discovered an extremely finely disperse mixture of α- and β-phases at the place of contact of the fused layer with the substrate. With all regimes of PLHT we found quenching cracks. After irradiation in liquid nitrogen we did not find any signs of crystalline structure. Microhardness of the layer is ∿H 980.

The results of metallographic analysis were not confirmed by x-ray diffraction analysis. Pulsed irradiation in air does not bring about any qualitative change of the phase composition of the alloy, i.e., we find α-, β-phases, the phase CdLi, and a small amount of $LiMgAl_2$. In addition to that we discovered two solid solutions on the basis of magnesium: α-Mg and α'-Mg (Table 1), which is a result of decomposition of supersaturated solid solution. Here we find stable and metastable solid solutions. Stable solid solution forms when a third phase segregates, but this phase was not revealed radiographically because of its small amount.

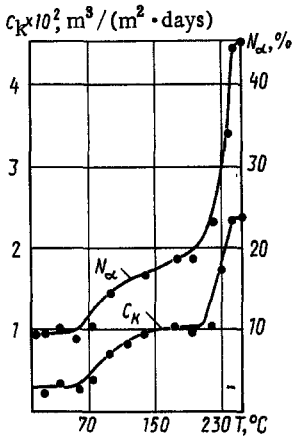

Fig. 9. Effect of the temperature to which alloy MA21 is preliminarily heated in continuous irradiation on the corrosion rate C_k and on the volume fraction of the α-phase N_α.

*Here and henceforth in the text hardness is given in MPa.

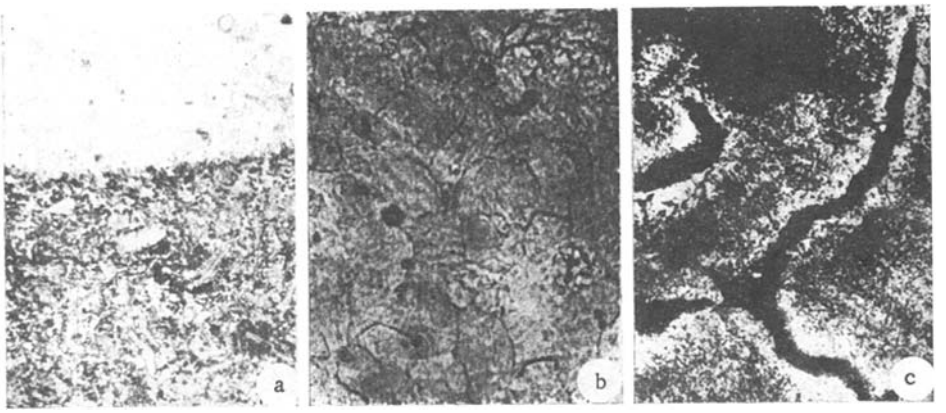

Fig. 10. Microstructure of alloy MA21 after pulsed irradiation (E = 15 J, d = 3 mm): a) in the transition zone; b) at the periphery of the pulse spot; c) in the zone of microcracks (center of the spot); a) ×100; b, c) ×300.

An analysis of the diffractograms of the alloy irradiated in liquid nitrogen showed that there is no biphase decomposition. Together with the lines of α- and β-phases we sometimes found a weak halo which indicates that there is an amorphous phase present. The lines of α- and β-phases on the diffractograms are due to the fact that x-rays penetrate to a greater depth than the thickness of single-phase solid solution or of the amorphous layer.

It was shown by x-ray spectroscopic analysis that the regularity of the change of concentration of the principal alloying elements after laser treatment is analogous to its change in the initial alloy. On account of the small size of the grains it is difficult to determine the composition of the phases in the fused zone. It was established that compared with the β-phase, the α-phase contained less cadmium (5.8 and 3.0%, respectively) and somewhat more zinc (0.7 and 1.4%, respectively). The β-phase contains finely disperse inclusions 1-2 μm in size, enriched with aluminum (up to 45%) and zinc (up to 11%). It is very difficult to determine the exact composition of the inclusions because of their small size and because it is impossible to analyze the content and establish the presence of lithium in them. After fusion by laser the distribution of elements is more uniform (within the limits of sensitivity of the method). After continuous and pulsed irradition the inclusions detected in the initial alloy were not found [3].

The results of corrosion tests of the alloy after CLHT and PLHT and subsequent heating are presented in Table 2. It can be seen that after continuous treatment the corrosion rate is 5-8 times lower, and after pulsed treatment 15-20 times lower than with the alloy in the initial state. However, irradiation with overlapping entails a corrosion rate of the alloy after PLHT approximately three times higher than after CLHT [5]. This is obviously due to the high concentrational nonuniformity in the zone of overlapping of the pulse spots caused by the difference in the phase composition of these zones and the compressive or tensile stresses in them which lead to the destruction of the protective oxide film. In connection with that the zones of overlapping become sections of intense anodic breakdown. With the methods of x-ray spectroscopic and metallographic analyses we did not reveal any qualitative difference in the structure of the track or in the zone of overlapping, and the application of transmission microscopy is difficult because alloy MA21 cannot be worked into foil.

In the zone of overlapping we found bad deterioration in the form of pitting after pulsed treatment. After CLHT there were no great differences between the microstructure in the tracks and zones of overlapping, nevertheless, some nonuniformity of etching does exist in these parts. However, after repeated additional heating the surface becomes more uniformly etched. Regardless of the fact that the corrosion rate is somewhat higher after repeated heating, the general state of the surface is more favorable. On the other hand, when alloy previously subjected to pulsed irradiation is heated, pitting at the places of overlapping is even more pronounced.

The results of microhardness measurement presented below showed that, as a rule, microhardness in the zone of overlapping is lower than directly in the spot or track:

Treatment	H
CLHT	
Without heating.....	710-760/720-780
160°C, 16 h	700-750/700-740
PLHT	
Without heating.....	800-890/900-940
160°C, 16 h.....	750-860/760-860

Note. The numerator contains microhardness in the zone of overlapping of spots or tracks, the denominator directly in the spot or track.

After heating, microhardness becomes more uniform over the surface. However, whereas heating after CLHT has a favorable effect, after PLHT it apparently increases concentrational nonuniformity and impairs corrosion resistance. This requires further detailed investigation.

The effect of laser treatment on the mechanical properties of the alloy MA21 was reported on in [4]. It should be noted that it is difficult to give a realistic evaluation of the strength of the alloy from standard specimens after CLHT and PLHT because in continuous treatment the tracks were made without overlapping, whereas the pulse spots had to be made with overlapping, i.e., in the latter case the effect of the overlapping zones of irradiation is considerable. In addition, as mentioned before, in the zone affected by the pulses microcracks originate, and they act as stress raisers.

The results of our investigation show that for industrial use the most favorable is the finely disperse quasieutectic structure obtained after CLHT. When solids are heated by laser, it becomes necessary to take into account the thermophysical and optical properties of the substances in dependence on the temperature, i.e., it is necessary to solve a thermal problem with nonlinearities of the first and second kind, which presents considerable difficulties [12]. The known methods, e.g., [8, 13], do not take into account the temperature to which a part may be heated in CLHT. Yet when parts are treated in air, taking ΔT_p into account makes it possible to determine the technological parameters of the process and to estimate its productivity.

Taking the experimentally obtained value of ΔT_p into account, we calculate the critical mass of the part at which the specified surface can be irradiated for a specified time with certain parameters of treatment without the structure and properties deviating from the specified ones. We adopt some assumptions: 1) the absorption coefficient before irradiation is constant; 2) the beam is shifted with sufficient speed over the surface and the thermal conductivity suffices for equalizing the temperature gradients in the bulk and on the surface.

The amount of heat which has to be supplied to the part of mass M and specific heat c so as to raise its temperature to ΔT can be determined by the equation

$$P=Mc\Delta T. \tag{2}$$

On the other hand, the amount of heat supplied to a part during CLHT in unit time is

$$P=WA\tau, \tag{3}$$

where W is the radiation intensity (W), A is the absorption coefficient, τ is the time during which the radiation acts (sec).

When we equate Eqs. (2) and (3), we obtain:

$$M=\frac{WA\tau}{c\Delta T}. \tag{4}$$

The time required for laser treatment of a part with surface S is determined by the width of the hardened "track" B, the speed with which the beam is shifted over the surface, and the coefficient of overlapping of the tracks m. In that case the productivity of the process is

$$Q=S/t=Bv/m \tag{5}$$

and the time is

$$t = Sm/Bv. \quad (6)$$

Hence, Eq. (4) can be presented in its final form:

$$M_{cr} = \frac{WASm}{c\Delta T_p 3v}, \quad (7)$$

where M_{cr} is the sought critical mass of the part.

The authors of [14, 15] investigated the effect of CLHT on the corrosion resistance of cast iron SCh-24 and of the aluminum alloy AL4. The dependence of the corrosion resistance (of the anodic current) of alloy AL4 on the power density of the radiation is analogous to the similar dependence applying to alloy MA21 with different energy contributions. This obviously makes it possible to apply the results of our investigations to other alloys of eutectic type.

Conclusions. 1. For the practical application of the alloy MA21 it is most favorable if it has a fine-grained quasieutectic structure obtained in continuous laser treatment.

2. Between the power density of the radiation, the geometry of the laser track, the corrosion rate, and the volume fraction of α-phase in the alloy MA21 there exist empirical correlations.

3. The permissible temperature interval to which the alloy MA21 may be heated in irradiation is ΔT_p = 60-70°C.

4. To eliminate the effect of nonsteady fluxes on the process of eutectic crystallization in CLHT in air, the wall thickness of parts must not be less than 30 mm.

5. A method of engineering calculation of the critical mass of the irradiated part was worked out; with it the parameters of the technological process of CLHT in air can be evaluated.

LITERATURE CITED

1. R. Kh. Kalimullin and Yu. Ya. Kozhevnikov, "The effect of laser treatment on the structure and corrosive properties of Mg—Li alloys," Metalloved. Term. Obrab. Met., No. 5, 18-21 (1985).
2. R. Kh. Kalimullin, V. V. Valuev, and A. T. Berdnikov, "The effect of surface laser treatment on the creep of the magnesium—lithium alloy MA21," Metalloved. Term. Obrab. Met., No. 9, 39-41 (1986).
3. R. Kh. Kalimullin and A. T. Berdnikov, "Improvement of the corrosion resistance of the magnesium—lithium alloy MA21 by surface laser treatment," Zashch. Met., 19, No. 3, 262 (1986).
4. R. Kh. Kalimullin, Yu. Ya. Kozhevnikov, I. Ya. Faizullin, and V. V. Valuev, "The effect of laser treatment on the structure and the mechanical properties of the alloy MA21," Metalloved. Term. Obrab. Met., No. 9, 31 (1984).
5. Inventors' Certificate No. 1262729.
6. V. I. Elagin, "Prediction of metastable phase diagrams," Metalloved. Legkikh Splavov, No. 1, 3 (1985).
7. K. M. Savitskii, Yu. V. Efimov, et al., The Metallurgy and Metal Science of Nonferrous Metals [in Russian], Naukova Dumka, Kiev (1982).
8. O. Yu. Kotsyubinskii, "Evaluation of the technological possibilities of hardening involving the use of continuous laser," Metalloved. Term. Obrab. Met., No. 1, 24-27 (1980).
9. A. A. Vedenov and G. G. Gladush, Physical Processes in Laser Treatment of Materials [in Russian], Énergoatomizdat, Moscow (1985).
10. N. N. Rykalin, A. A. Uglov, and A. N. Kokora, Laser Treatment of Materials [in Russian], Mashinostroenie, Moscow (1975).
11. Yu. A. Taran and M. N. Mazur, The Structure of Eutectic Alloys [in Russian], Metallurgiya, Moscow (1978).
12. N. N. Rykalin and A. A. Uglov, "The effect of concentrated energy fluxes on materials. Problems and prospects," Fiz. Khim. Obrab. Mater., No. 5, 3 (1983).

13. S. F. Moryashchev, A. A. Kislitsyn, and F. K. Kosyrev, "Optimization of the parameters of the process of hardening steel by the radiation of a CO_2-laser," Fiz. Khim. Obrab. Mater., No. 1, 94 (1984).
14. Yu. V. Vasil'ev, N. V. Edneral, T. G. Kuz'menko, et al., "The effect of laser treatment on the corrosion properties of cast iron SCh-24 and steel U10," Zashch. Met., 18, No. 3, 450 (1982).
15. B. K. Opara, V. M. Andriyakhin, V. I. Volgin, and V. V. Bandurkin, "The corrosive behavior of the aluminum alloy AL4 strengthened by the radiation of the CO_2-laser," Zashch. Met., 18, No. 1, 87 (1985).

SURFACE ALLOYING OF ALLOY AL25 BY LASER

I. V. Bogolyubova, I. F. Deriglazova, and B. F. Mul'chenko

UDC 621.9.048:669.717

The literature at present deals fairly extensively with questions of laser alloying of iron-carbon alloys. The special features of strengthening aluminum alloys by introducing alloying elements into the surface layer with the aid of laser radiation were investigated much less. The authors of [1, 2] presented the results of investigations into the possibility of alloying aluminum alloys with the aid of pulsed laser radiation.

The object of the present work is the investigation of the peculiarities of structure formation in the surface layer of alloy AL25 when it is alloyed with wear-resistant compositions with the aid of a continuous CO_2 laser, and the discovery of the basic possibility of carrying out the process of laser alloying of the grooves for the compression rings in pistons of internal combustion engines made of this alloy.

Specimens with 90-mm diameter of alloy AL25 (12% Si, 1.1% Mg, 1.3% Cu, 1.0% Ni) [3] with initial structure of α-solid solution and eutectic (Fig. 1a) were treated by CO_2 lasers with power density $4\cdot10^3$-10^4 W/cm^2; the specimen was shifted at a speed of 0.1-0.5 m/min. The treatment was carried out in an atmosphere of protective gases. The structure of the alloy in the initial state and after laser alloying was investigated on microscopes MIM-8 and "Neophot." The distribution of the alloying elements was determined on a scanning electron microscope JSM-35 with an attachment for x-ray spectroscopic analysis. Microhardness was measured on an instrument PMT-3 with a load of 0.196 N.

For alloying we used powders on the basis of NiCr, FeCuB, NiCrMo which, in the form of coatings, were applied to the surface of the aluminum alloy, and then they were fused with the aid of laser radiation.

In consequence of the high cooling rate in crystallization, the α-solid solution and the eutectic become refined in the fused layer, a finely disperse structure forms (Fig. 1b). Moreover, the addition of alloying elements to the surface layer leads to the formation of metastable solid solution supersaturated with the added elements [4]. As a result the

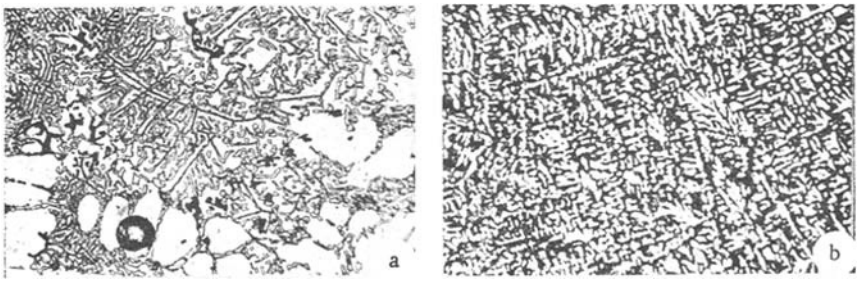

Fig. 1. Microstructure of the alloy AL25 in the initial state (a) and after laser alloying with nickel and chromium (b). ×200.

Scientific and Production Association "NIITavoprom." Translated from Metallovedenie i Termicheskaya Obrabotka Metallov, No. 5, pp. 24-25, May, 1988.

 0026-0673/88/0506-0348$12.50